On the numerical approximation of the K-epsilon turbulence model for two dimensional compressible flows

Christian Olivier, Bernard Larrouturou

UNITÉ DE RECHERCHE
INRIA-SOPHIA ANTIPOLIS

Institut National
de Recherche
en Informatique
et en Automatique

Domaine de Voluceau
Rocquencourt
B.P.105
78153 Le Chesnay Cedex
France
Tél.:(1) 39 63 55 11

Rapports de Recherche

N° 1526

Programme 6
Calcul Scientifique, Modélisation et
Logiciel numérique par Ordinateur

ON THE NUMERICAL APPROXIMATION OF THE K-ε TURBULENCE MODEL FOR TWO DIMENSIONAL COMPRESSIBLE FLOWS

Christian OLIVIER
Bernard LARROUTUROU

Septembre 1991

RR-1526

ON THE NUMERICAL APPROXIMATION OF THE K-$\mathcal{E}$ TURBULENCE MODEL FOR TWO DIMENSIONAL COMPRESSIBLE FLOWS

Christian OLIVIER[1]

Bernard LARROUTUROU[2]

(1)INRIA Sophia-Antipolis 2004,route des Lucioles
06560 Valbonne(FRANCE)

(2)CERMICS, INRIA Sophia-Antipolis 2004,route
des Lucioles 06560 Valbonne(FRANCE)

ON THE NUMERICAL APPROXIMATION OF THE K-$\mathcal{E}$ TURBULENCE MODEL FOR TWO-DIMENSIONAL COMPRESSIBLE FLOWS

C. OLIVIER[1], B. LARROUTUROU[2]

(1) INRIA, Sophia-Antipolis, 06560 VALBONNE, FRANCE
(2) CERMICS, INRIA, Sophia-Antipolis, 06560 VALBONNE, FRANCE

ABSTRACT: We present in this report a numerical method for solving the k-ϵ turbulence model without "wall-law" for two-dimensional compressible flows. This method combines an upwind finite-volume approximation for the inviscid terms and a centered finite-element for the viscous terms and the source term. As an illustration of our method, we present the test-case of a compressible subsonic mixing layer.

APPROXIMATION NUMERIQUE DU MODELE DE TURBULENCE K-$\mathcal{E}$ POUR DES ECOULEMENTS COMPRESSIBLES BIDIMENSIONNELS

C. OLIVIER[1], B. LARROUTUROU[2]

(1) INRIA, Sophia-Antipolis, 06560 VALBONNE, FRANCE
(2) CERMICS, INRIA, Sophia-Antipolis, 06560 VALBONNE, FRANCE

RESUME: Nous présentons dans ce rapport une méthode numérique de résolution du modèle de turbulence k-ϵ sans loi de paroi pour des écoulements compressibles bidimensionnels. Cette méthode combine une approximation décentrée de type volumes finis pour les termes non visqueux et une approximation centrée de type éléments finis pour les termes visqueux ainsi que pour le terme source. Le cas-test choisi pour illustrer notre méthode est celui d'une couche de mélange compressible subsonique.

Contents

INTRODUCTION

TVD techniques have undoubtedly enriched the set of methods available for computing external aerodynamics, improving the robustness of the methods and allowing some efficient implicit relaxation schemes, at least for upwind TVD approximation (see for example [18], [19]) ; it is then easier to compute compressible transonic and supersonic flows in a conservative way. Simultaneously with this progress, compressible turbulent models are better understood. It is then important to study how TVD methods can be extended to compressible turbulence models, and in particular when additional equations are introduced.

The work presented in this report is a premilinary step towards the numerical solution of the classical k-ϵ turbulence model for two-dimensional turbulent compressible flows in the framework of the upwind conservative finite-element method developed in our group for the solution of the Euler equations (see [3], [4], [5]).

We concentrate below on the spatial approximation and time integration of the six partial differential equations which form the two-dimensional k-ϵ model. In our formulation, the first-order spatial derivatives (that is, the spatial derivatives appearing in the Euler equations for the density, momentum and energy equations, and the convective terms of the k and ϵ equations) are evaluated using a conservative limited second-order accurate upwind scheme, namely a maximum-preserving extension of Roe's approximate Riemann solver [13] ; the diffusive terms are computed in the same way as in the classical P1 finite-element method.

We do not address here the question of the numerical approximation of the nonlinear "wall-laws" which are usually coupled with the k-ϵ model; this problem will be studied in a later work.

The time integration of the model also rises some difficulties. Indeed, our investigation of a simple one-dimensional model problem shows (in Section 3 below) that an implicit method has to be used for an efficient solution of the considered steady problem. This problem of implicit stepping has been studied in an early work of Vandromme [15] for an upwind flux–splitted finite–volume method. We compare here several implicit treatments of the proposed maximum preserving scheme in the one-dimensional context, and then extend one of them, a linearized implicit method, to the two-dimensional case.

We conclude the report by showing in Section 5 some results of a calcu-

lation on a two-dimensional test-case with no wall, namely a compressible subsonic mixing layer.

1 GOVERNING EQUATIONS

1.1 The basic model

We write the two-dimensional compressible Navier-Stokes equations extended with the $k-\epsilon$ turbulence model in normalized conservative form as follows:

$$\begin{aligned}&\frac{\partial W}{\partial t}+\frac{\partial F(W)}{\partial x}+\frac{\partial G(W)}{\partial y}=\\&\quad\frac{1}{Re}\left(\frac{\partial R(W)}{\partial x}+\frac{\partial S(W)}{\partial y}\right)+\frac{\partial \frac{1}{R_t}\tilde{R}(W)}{\partial x}+\frac{\partial \frac{1}{R_t}\tilde{S}(W)}{\partial y}+\Omega(W)\,,\end{aligned}\tag{1}$$

for $t\geq 0$ and (x,y) in $\mathcal{D}$, a bounded domain of $\mathbb{R}^2$ with boundary $\partial\mathcal{D}=\Gamma$. In (1), $W(x,y,t)$ is a vector function in $\mathbb{R}^6$, whose components are the conservative variables:

$$W=\begin{pmatrix}\rho\\ \rho u\\ \rho v\\ E\\ \rho k\\ \rho\epsilon\end{pmatrix}\;;\tag{2}$$

here and in the sequel, ρ denotes the fluid density, u and v are the components of the velocity, E is the total energy per unit volume, k is the kinetic energy of turbulence and ϵ is its dissipation rate.

In (1), $F(W)$ and $G(W)$ are the convective and acoustic fluxes (which we will also sometimes call the "Euler fluxes" or "hyperbolic fluxes"): given by:

$$F(W)=\begin{pmatrix}\rho u\\ \rho u^2+p\\ \rho uv\\ (E+p)u\\ \rho uk\\ \rho u\epsilon\end{pmatrix}\quad,\quad G(W)=\begin{pmatrix}\rho v\\ \rho uv\\ \rho v^2+p\\ (E+p)v\\ \rho vk\\ \rho v\epsilon\end{pmatrix}\,,$$

where the total energy and the pressure are expressed by:

$$E = \rho C_v T + \frac{1}{2}\rho(u^2 + v^2) + \rho k \ , \tag{3}$$

and

$$p = (\gamma - 1)\rho C_v T \ . \tag{4}$$

Here, γ is the (constant) specific heat ratio ($\gamma = 1.4$ for a perfect diatomic gas).

Next, the diffusive laminar fluxes $R(W)$ and $S(W)$ are defined as follows:

$$R(W) = \begin{pmatrix} 0 \\ \tau_{xx} \\ \tau_{xy} \\ u\,\tau_{xx} + v\,\tau_{xy} + \dfrac{\gamma\,\kappa}{Pr}\dfrac{\partial e}{\partial x} \\ \dfrac{\partial k}{\partial x} \\ \\ \dfrac{\partial \epsilon}{\partial x} \end{pmatrix} \ , \quad S(W) = \begin{pmatrix} 0 \\ \tau_{xy} \\ \tau_{yy} \\ u\,\tau_{xy} + v\,\tau_{yy} + \dfrac{\gamma\,\kappa}{Pr}\dfrac{\partial e}{\partial y} \\ \dfrac{\partial k}{\partial y} \\ \\ \dfrac{\partial \epsilon}{\partial y} \end{pmatrix} \ ,$$

and the turbulent diffusive fluxes $\tilde{R}(W)$ and $\tilde{S}(W)$ are given by:

$$\tilde{R}(W) = \begin{pmatrix} 0 \\ -\frac{2}{3}\rho\,k\,R_t + \tau_{xx} \\ \tau_{xy} \\ -\frac{2}{3}\rho\,k\,u\,R_t + u\,\tau_{xx} + v\,\tau_{xy} + \dfrac{\gamma\,\mu}{P_t}\dfrac{\partial e}{\partial x} \\ \dfrac{1}{\sigma_k}\dfrac{\partial k}{\partial x} \\ \dfrac{1}{\sigma_\epsilon}\dfrac{\partial \epsilon}{\partial x} \end{pmatrix} \ ,$$

$$\tilde{S}(W) = \begin{pmatrix} 0 \\ \tau_{xy} \\ -\frac{2}{3}\rho\,k\,R_t + \tau_{yy} \\ -\frac{2}{3}\rho\,k\,v\,R_t + u\,\tau_{xy} + v\,\tau_{yy} + \dfrac{\gamma\,\mu}{P_t}\dfrac{\partial e}{\partial y} \\ \dfrac{1}{\sigma_k}\dfrac{\partial k}{\partial y} \\ \dfrac{1}{\sigma_\epsilon}\dfrac{\partial \epsilon}{\partial y} \end{pmatrix} \ .$$

In these expressions, e is the specific internal energy ($e = C_v T$), the terms proportional to $\frac{2}{3}\rho k$ come from a diagonal term $\frac{2}{3}\rho k\, Id$ in the formulation of the Reynolds stress tensor (see e.g. [15]), and τ_{xx}, τ_{xy} and τ_{yy} are the components of the viscous stress tensor:

$$\tau_{xx} = \frac{2}{3}\mu\left(2\frac{\partial u}{\partial x} - \frac{\partial v}{\partial y}\right),$$

$$\tau_{yy} = \frac{2}{3}\mu\left(2\frac{\partial v}{\partial y} - \frac{\partial u}{\partial x}\right),$$

$$\tau_{xy} = \mu\left(\frac{\partial u}{\partial y} + \frac{\partial v}{\partial x}\right).$$

Here, μ and κ are the normalised gas viscosity and the normalised thermal conductivity respectively; in the general case, these coefficients are functions of the temperature (for example $\mu(T)$ given by Sutherland's law [1]); but for the sake of simplicity we consider here that these two coefficients are constant (and equal to 1 since normalised).

Two nondimensional numbers appear in the previous equations. The first one is the Reynolds number Re which measures the importance of inertial strengths compared to viscous strengths, given by:

$$Re = \frac{\rho_0 U_0 L_0}{\mu_0},$$

where ρ_0, U_0, L_0 and μ_0 are respectively the density unit, the velocity unit, the length unit chosen to nondimensionalize the equations and the (dimensionalized) gas viscosity. The second one is the Prandtl number Pr which only depends on the physical characteristics of the fluid:

$$Pr = \frac{\mu_0 C_p}{\kappa_0},$$

C_p being the specific heat at constant pressure (C_p is supposed constant), and κ_0 the (dimensionalized) thermal conductivity.

The turbulent Reynolds number R_t which appears in (1) comes from the definition of the eddy viscosity μ_t in the $k-\epsilon$ turbulence model:

$$R_t = \frac{1}{\mu_t}, \quad \mu_t = \frac{c_\mu\, \rho\, k^2}{\epsilon}.$$

Moreover, the turbulent Prandtl number P_t appearing in the turbulent diffusive fluxes $\tilde{R}(W)$ and $\tilde{S}(W)$ is simply taken equal to the Prandtl number Pr (we take $Pr = 0.72$ in all calculations below).

Lastly, the source term Ω in (1) is given by:

$$\Omega(W) = \begin{pmatrix} 0 \\ 0 \\ 0 \\ 0 \\ -\rho\,\epsilon + \mathcal{P} \\ c_{\epsilon_1}\dfrac{\epsilon}{k}\,\mathcal{P} - c_{\epsilon_2}\dfrac{\rho\,\epsilon^2}{k} \end{pmatrix} .$$

The production term $\mathcal{P}$ is defined as:

$$\mathcal{P} = \mathcal{A}.\mathcal{B} ,$$

with:

$$\mathcal{A} = \begin{pmatrix} \dfrac{1}{R_t}\left(2\dfrac{\partial u}{\partial x} - \dfrac{2}{3}\left(\dfrac{\partial u}{\partial x} + \dfrac{\partial v}{\partial y}\right)\right) - \dfrac{2}{3}\rho\,k & \dfrac{1}{R_t}\left(\dfrac{\partial u}{\partial y} + \dfrac{\partial v}{\partial x}\right) \\ \dfrac{1}{R_t}\left(\dfrac{\partial u}{\partial y} + \dfrac{\partial v}{\partial x}\right) & \dfrac{1}{R_t}\left(2\dfrac{\partial v}{\partial y} - \dfrac{2}{3}\left(\dfrac{\partial u}{\partial x} + \dfrac{\partial v}{\partial y}\right)\right) - \dfrac{2}{3}\rho\,k \end{pmatrix} ,$$

and:

$$\mathcal{B} = \begin{pmatrix} \dfrac{\partial u}{\partial x} & \dfrac{\partial v}{\partial x} \\ \dfrac{\partial u}{\partial y} & \dfrac{\partial v}{\partial y} \end{pmatrix} ,$$

that is:

$$\mathcal{P} = \frac{1}{R_t}\left(2\frac{\partial u}{\partial x}^2 - \frac{2}{3}\left(\frac{\partial u}{\partial x} + \frac{\partial v}{\partial y}\right)^2 + \left(\frac{\partial v}{\partial x} + \frac{\partial u}{\partial y}\right)^2 + 2\frac{\partial v}{\partial y}^2\right) - \frac{2}{3}\rho\,k\left(\frac{\partial u}{\partial x} + \frac{\partial v}{\partial y}\right) .$$

All constants in the model take their classical values (these constants have been calibrated by numerical experiments in the incompressible case; see e.g.[10]):

$$c_\mu = 0.09 , \quad c_{\epsilon_1} = 1.44 , \quad c_{\epsilon_2} = 1.92 , \quad \sigma_k = 1 , \quad \sigma_\epsilon = 1.3 .$$

1.2 The change of variable

Apart from the influence of the "turbulence variables" k and ϵ on the "flow variables" ρ, ρu, ρv, E through the turbulent viscosity μ_t, there is a coupling between these two sets of variables even at the level of the hyperbolic fluxes F and G since the turbulent kinetic energy ρk appears in the expression (3) of the total energy E. In the present form, this fact prevents us from treating these hyperbolic terms in the same way as in the laminar case (that is, using an approximate Riemann solver, as we will explain below; this is the reason why the term ρk is sometimes omitted in the energy equation(see e.g. [12]). Here, we will solve this difficulty by introducing an appropriate change of variables.

Combining the equations giving the pressure and the total energy, we obtain:

$$p = (\gamma - 1)\left(E - \frac{1}{2}\rho(u^2 + v^2) - \rho\, k\right) .$$

We set then:

$$p' = p + \frac{2}{3}\rho\, k \ ;$$

consequently, we get:

$$p' = (\gamma - 1)\left(E - \frac{1}{2}\rho(u^2 + v^2) + \beta\, \rho\, k\right) ,$$

where:

$$\beta = -1 + \frac{2}{3\,(\gamma - 1)} .$$

Finally, setting:

$$E' = E + \beta\, \rho\, k \ ,$$

we see that the relation linking p' and E' has the classical form:

$$p' = (\gamma - 1)\left(E' - \frac{1}{2}\rho(u^2 + v^2)\right) ,$$

and that, taking out the terms $\frac{2}{3}\rho\, k$ in the expression of the turbulent viscous stress $\tilde{R}$ and $\tilde{S}$ and incorporating them in the fluxes $F(W)$ and $G(W)$, we obtain for the hyperbolic terms of the conservation equation for the modified energy E' the following classical expressions:

$$E'_t + [u(E' + p')]_x + [v(E' + p')]_y = RHS \ .$$

To summarize, the model we will actually solve numerically still has the same form as system (1):

$$\begin{aligned}&\frac{\partial W}{\partial t}+\frac{\partial F(W)}{\partial x}+\frac{\partial G(W)}{\partial y}=\\&\frac{1}{Re}\left(\frac{\partial R(W)}{\partial x}+\frac{\partial S(W)}{\partial y}\right)+\frac{\partial \frac{1}{R_t}\tilde{R}(W)}{\partial x}+\frac{\partial \frac{1}{R_t}\tilde{S}(W)}{\partial y}+\Omega(W)\ .\end{aligned}\tag{5}$$

The vectors on the left-hand side are now defined as:

$$W=\begin{pmatrix}\rho\\ \rho u\\ \rho v\\ E'\\ \rho k\\ \rho\epsilon\end{pmatrix}\ ,\quad F(W)=\begin{pmatrix}\rho u\\ \rho u^2+p'\\ \rho uv\\ (E'+p')\,u\\ \rho uk\\ \rho u\epsilon\end{pmatrix}\ ,\quad G(W)=\begin{pmatrix}\rho v\\ \rho uv\\ \rho v^2+p'\\ (E'+p')\,v\\ \rho vk\\ \rho v\epsilon\end{pmatrix}\ ,\tag{6}$$

with the classical expression (7) of the pressure p':

$$p'=(\gamma-1)\left(E'-\frac{1}{2}\rho(u^2+v^2)\right)\ ;\tag{7}$$

moreover, the vectors in the right-hand side of (5) are identical to the corresponding vectors in the right-hand side of (1), except the turbulent viscous stress vectors $\tilde{R}$ and $\tilde{S}$ where the terms proportional to $\frac{2}{3}\rho k$ should now be omitted. This change of variables therefore has the advantage that we now have the usual expressions for the hyperbolic part (6)-(7) of the model.

2 ONE-DIMENSIONAL STUDY

Our objective in this section is to address the difficulties related to the approximation of the source terms in the equations of k and ϵ, and to compare several approaches for solving these difficulties. To this aim, we will consider a simplified one-dimensional problem, in which we do not take the influence of the turbulence variables k and ϵ on the flow variables ρ, u, v, p into account and neglect the diffusive terms. This problem will first be solved by a space-marching method, which is specially well adapted to the simple case under consideration, and by several (explicit or implicit) time integration methods, which we will compare before extending some of them for the approximation of the complete two-dimensional model.

2.1 The simplified model

The simplified model considered in this section rests on the following (irrealistic) assumptions: we suppose that the flow is one-dimensional in the domain $\{0 \leq x \leq 1\}$, that the density is constant ($\rho = 1$), and that the components of the gas velocity are given by:

$$u = u(x) = 1.1 - x \ , \quad v = 0 \ .$$

Thus, as sais above, we put the emphasis on the numerical treatment of the turbulence source term by simply considering the following system for the turbulence variables k and ϵ (we set $\vec{V} = (u, v)$):

$$\left\{ \begin{array}{l} k_t + div(\rho k \vec{V}) = \Omega_k \ , \\ \epsilon_t + div(\rho \epsilon \vec{V}) = \Omega_\epsilon \ ; \end{array} \right. \tag{8}$$

here, Ω_k and Ω_ϵ are the components of the source term Ω given in the previous section. We will solve this problem on the domain $\{x \in [0,1], \ t \geq 0\}$, with the initial data:

$$k(x,0) = k_0 = 10^{-4} \ , \quad \epsilon(x,0) = \epsilon_0 = 9 \ 10^{-6} \ ,$$

so that $\mu_t = 10^{-4}$, and the boundary conditions:

$$k(0,t) = k_0 \ , \quad \epsilon(0,t) = \epsilon_0 \ .$$

2.2 Steady problem

Before comparing several methods for the solution of the time-dependent system (8), we are going to solve the corresponding steady system (which is hyperbolic in space since $u > 0$) using a space marching method. Setting:

$$W = \left(\begin{array}{c} k \\ \epsilon \end{array} \right) \ ,$$

we rewrite the steady system as the following first-order vector ordinary differential equation:

$$\frac{\partial}{\partial x}(uW) = \Omega(W) \ .$$

Since $u_x = -1$, the steady system takes the form:

$$\frac{\partial}{\partial x} W = \frac{\Omega(W)}{u} + W \ ,$$

and we simply solve this system using the classical fourth-order

We made several calculations for different mesh sizes Δx. The results show that there is no appreciable difference between the numerical solutions obtained with $\Delta x = 10^{-4}$ and $\Delta x = 10^{-3}$, and that the solution obtained with $\Delta x = 10^{-2}$ is very close to the latter (see Figure 1).

Thus, the space marching Runge-Kutta method gives us a reference steady solution, and allows us to determine the appropriate mesh spacing to be used for studying the time-dependent methods below: we choose to use 101 points in the calculations below.

2.3 Solution of the time-dependent problem by an explicit method

Now we solve the time-dependent system (8) using an upwind explicit method (which we will later extend to two space dimensions).

2.3.1 The numerical scheme

With the same notations as above, we rewrite system (8) as:

$$\frac{\partial W}{\partial t} + \frac{\partial}{\partial x} F(W) = \Omega \ , \tag{9}$$

with $F(W) = uW$. We write the general form of an explicit conservative approximation of (9) as:

$$mes(C_j) \frac{W_j^{n+1} - W_j^n}{\Delta t} + \Phi_{j+\frac{1}{2}}^n - \Phi_{j-\frac{1}{2}}^n = mes(C_j) \Omega \left(W_j^n \right) \ ; \tag{10}$$

in this relation, the cell C_j denotes the interval $[x_{j-\frac{1}{2}}, x_{j+\frac{1}{2}}]$ around mesh point x_j, with $x_{j+\frac{1}{2}} = \dfrac{x_j + x_{j+1}}{2}$, and the numerical flux $\Phi_{j+\frac{1}{2}}^n$ approximates $F\left(W_{j+\frac{1}{2}}^n \right)$.

As the velocity u is positive, a first-order accurate upwind scheme is very simply obtained by setting $\Phi^n_{j+\frac{1}{2}} = u_j W^n_j$; the scheme writes:

$$W^{n+1}_j = W^n_j - \frac{\Delta t}{mes\,(C_j)} \left(u_j\, W^n_j - u_{j-1}\, W^n_{j-1} \right) + \Delta t\, \Omega \left(W^n_j \right) \ . \qquad (11)$$

Following the MUSCL approach of van Leer [17], we can construct a limited second-order approximation by setting:

$$\Phi^n_{j+\frac{1}{2}} = u_j \left(W_j + \frac{mes\,(C_j)}{2} (W_x)^n_j \right) \ , \qquad (12)$$

where $(W_x)^n_j$ approximates the gradient of W in the cell C_j at time $t^n = n\Delta t$. In order to preserve monotonicity, we use the following "limited slope", introduced by van Albada and van Leer [16]:

$$(W_x)^n_j = Moy \left(\frac{W^n_j - W^n_{j-1}}{x_j - x_{j-1}}; \frac{W^n_{j+1} - W^n_j}{x_{j+1} - x_j} \right) \ ,$$

with:

$$\begin{cases} Moy\,(a;b) = \dfrac{\left(a^2 + \alpha\right) b + \left(b^2 + \alpha\right) a}{a^2 + b^2 + \alpha} & \text{if } a \text{ and } b \text{ have the same sign} \\ 0 & \text{if not} \end{cases}$$

(the small positive constant α prevents the zero divide)

In summary, we have now derived an explicit scheme which is first-order accurate in time and "quasi-second-order" in space.

2.3.2 Numerical results

We present on Figure 2 the stationnary solution obtained after convergence using the first- and second-order accurate schemes with 101 equally spaced points, and compare them with the steady solution obtained with the fourth-order Runge-Kutta method. The differences between first- and second-order accurate results are slight. One can note however that the fastest convergence for the first-order accurate scheme has been obtained for a CFL number $(\frac{u_{max}\Delta t}{\Delta x})$ of 1.03, whereas the best convergence for the second-order accurate

scheme is observed with a CFL number of 0.4 (see Figures 3 and 4, where we have plotted the residual:

$$Res^n = \sqrt{\sum_j mes\,(C_j) \left(\frac{W_j^{n+1} - W_j^n}{\Delta t} \right)^2}$$

as a function of the number of time steps n). The fact that the maximal admissible value of the CFL number exceeds 1 for this particular problem with the first-order accurate scheme comes from the presence of the source term, which is not taken into account in the classical stability analysis that predicts the usual condition $CFL \leq 1$.

2.4 Solution of the time-dependent problem by implicit methods

Lastly, we consider the solution of the one-dimensional problem (8) using two implicit formulations.

2.4.1 The linearized implicit scheme

Starting from the following semi-discrete expression of a (first-order accurate) fully implicit scheme:

$$\frac{W^{n+1} - W^n}{\Delta t} + \frac{\partial}{\partial x} \left[F\left(W^{n+1}\right) \right] = \Omega\left(W^{n+1}\right) , \tag{13}$$

and linearising $F(W^{n+1})$ and $\Omega(W^{n+1})$ about W^n, we obtain the following linearized implicit scheme in δ-form:

$$\begin{aligned} (Id - \Delta t \Omega'(W^n)) \;\; & (W^{n+1} - W^n) + \Delta t \frac{\partial}{\partial x} (u[W^{n+1} - W^n]) \\ & = \Delta t \left(\Omega(W^n) - \frac{\partial}{\partial x} (u\, W^n) \right) . \end{aligned} \tag{14}$$

For the fully discrete scheme, following [6], we use the spatially second-order accurate approximation described in the previous section to evaluate the explicit term, which controls the accuracy of the steady-state solution, and simply use the first-order accurate approximation of the convective term

for the implicit phase which only acts as a preconditioner . This gives the following finite-volume formula:

$$\left(\left(1+\frac{u_j\Delta t}{mes\,(C_j)}\right)Id-\Delta t\,\Omega'\left(W_j^n\right)\right)\delta W_j-\frac{u_{j-1}\Delta t}{mes\,(C_j)}\delta W_{j-1}=$$
$$\Delta t\Omega\left(W_j^n\right)-\frac{\Delta t}{mes\,(C_j)}\left(\Phi_{j+\frac{1}{2}}-\Phi_{j-\frac{1}{2}}\right)\ .$$

where $\delta W_j = W_j^{n+1} - W_j^n$ and where $\Phi_{j+\frac{1}{2}}$ is the previously defined second-order accurate flux. It is easy to see that the linear system to be solved at each time step for this simple one-dimensional spatially hyperbolic problem involves a bi-diagonal matrix which can be inverted by a single direct sweep in the direction of increasing x.

A straightforward stability analysis with a linear source term (which we omit here; see [7]) shows that this linearized implicit scheme is unconditionnally stable.

2.4.2 Numerical results

In addition to the above linearized implicit scheme, we have also studied two semi-implicit schemes, that is (a) explicit convection and linearized implicit source term, and (b) linearized implicit convection and explicit source term. The convergence histories of these two semi-implicit schemes are compared with those of the explicit and linearized fully implicit schemes for a CFL number of 1 on Figure 5. Examining the first 80 time-steps show that all four methods are time-consistent, whereas we see from the hundredth time step that the schemes which explicitly treat the convection term give the steady solution of this simple problem in a finite number of time steps.

To illustrate the efficiency of the implicit scheme, we compare on Figure 6 the convergence histories of the explicit scheme and of the linearized implicit scheme, with a CFL number which progressively increases from 17 to 16 10^6 . The gain in computer time for the computation of the steady solution clearly appears.

2.4.3 The nonlinear implicit scheme

We have also solved the nonlinear fully implicit formulation scheme (13) using Newton's method. It appears then that convergence to steady state is

reached after two time steps. However, solving the nonlinear system at each of the two time steps requires many Newton's iterations, and which eventually makes the nonlinear implicit method more costly than the linearized implicit scheme.

2.5 Conclusions

We have solved the simplified problem (8) with three several different methods, including a space-marching technique, and explicit and implicit time-integration schemes. The linearized Euler implicit method written in δ-form with a second-order half-upwind scheme in the explicit phase combined with a first-order upwind implicit preconditioner was found to be the most efficient time-integration method. We have observed, in particular, that this method allows us to use time-steps 10^5 greater than with the explicit method, independently of the mesh size; it is then possible to reach the steady-state solution with less than 30 time steps for the considered model problem. The nonlinear Euler implicit method allows us to obtain the steady-state solution after two time steps, but this method is very expensive in CPU-time.

3 THE TWO-DIMENSIONAL NUMERICAL APPROXIMATION

In view of the above conclusions, we will now extend the linearized implicit upwind method to the calculation of two-dimensional turbulent flows. The method presented below relies on our previous works on the approximation of the compressible Euler and laminar Navier-Stokes equations (see [2], [3], [4], [5], [6]). It operates on a (possibly unstructured) finite-element triangulation, and uses a MUSCL upwind formulation for the hyperbolic terms.

3.1 Spatial approximation

We will only briefly describe the main features of the approximation scheme, referring to e.g. [5] for more details.

Starting from a classical finite-element triangulation of the computational domain $\mathcal{D}$, we associate with all node S_i a cell C_i defined by joining succes-

sively the centroids of all triangles having S_i as a vertex and the mid-points of all segments stemmed from S_i (see Figure 7).

Now, we use a mixed finite-element / finite volume approximation. Denoting ϕ_i the usual piecewise linear finite-element basis function, it is easy to check that the relation $\iint_{C_i} dxdy = \iint_{\mathcal{D}} \phi_i \, dxdy$ holds. We will then derive our numerical scheme from the following formulation:

$$\iint_{C_i} (W_t + F_x + G_y) \, dxdy = \iint_{\mathcal{D}} \left(R_x + S_y + \left(\frac{\tilde{R}}{R_t}\right)_x + \left(\frac{\tilde{S}}{R_t}\right)_y + \Omega \right) \phi_i \, dxdy \tag{15}$$

Let us add a few remarks about this formulation. As far as the time derivative and diffusive terms are concerned, (15) is nothing but the so-called mass-lumped finite-element approximation of system (5). Moreover, it is easy to check that we would not modify the scheme (15) if we substitute a finite-volume approximation

$$\iint_{C_i} \left(R_x + S_y + \left(\frac{\tilde{R}}{R_t}\right)_x + \left(\frac{\tilde{S}}{R_t}\right)_y \right)$$

(approximated using Green's formula with piecewise linear approximations of the variables, see e.g. [2], [8]) instead of the finite-element integral

$$\iint_{\mathcal{D}} \left(R_x + S_y + \left(\frac{\tilde{R}}{R_t}\right)_x + \left(\frac{\tilde{S}}{R_t}\right)_y \right) \phi_i \, dxdy$$

for the diffusive terms. For the source term however, it is more natural to evaluate the finite-element integral $\iint_{\mathcal{D}} \Omega \phi_i \, dxdy$ instead of the mass-lumped term $\iint_{C_i} \Omega \, dxdy$ since this term contains spatial derivatives of the velocity.

It remains to describe the evaluation of the integral in the left-hand side of system (15). We simply use a one-point integration formula for the time derivative term, writing:

$$\iint_{C_i} W_t \, dxdy = area(C_i) \, \frac{W_i^{n+1} - W_i^n}{\Delta t} \, .$$

For the hyperbolic terms, we use Green's formula to get:

$$\iint_{C_i} (F_x + G_y) \, dxdy = \int_{\partial C_i} (F\nu_x + G\nu_y) = \sum_{S_j \in \mathcal{N}(i)} \int_{\partial C_i \cup \partial C_j} (F\nu_x + G\nu_y) \, ,$$

where $\vec{\nu} = (\nu_x, \nu_y)$ is the outward unit normal on the boundary ∂C_i of the cell C_i, and where $\mathcal{N}(i)$ is the set of all vertices which are neighbours of node S_i. The fluxes $\int_{\partial C_i \cup \partial C_j} (F\nu_x + G\nu_y)$ are evaluated for each segment $[S_i S_j]$ using Roe's approximate Riemann solver. The extension of this solver, originally defined for the Euler equations, to the complete system, i.e. to the equations of k and ϵ, is done by using the positivity-preserving multi-component Riemann flux proposed by B. Larrouturou [9]. This leads to very simple expressions: calling Φ_{ij}^{ρ} the component of the numerical flux for the density (given by Roe's approximate Riemann solver), we evaluate the first-order accurate components $\Phi_{ij}^{\rho k}$ and $\Phi_{ij}^{\rho \epsilon}$ of the convective fluxes corresponding to the two last variables ρk and $\rho \epsilon$ by the relations:

$$\Phi_{ij}^{\rho k} = \Phi_{ij}^{\rho} \times \begin{cases} k_i & \text{if } \Phi_{ij}^{\rho} > 0 \ , \\ k_j & \text{otherwise} \ , \end{cases} \tag{16}$$

$$\Phi_{ij}^{\rho \epsilon} = \Phi_{ij}^{\rho} \times \begin{cases} \epsilon_i & \text{if } \Phi_{ij}^{\rho} > 0 \ , \\ \epsilon_j & \text{otherwise} \ . \end{cases} \tag{17}$$

Spatially second-order accurate approximations of the hyperbolic terms are again obtained by considering that the variables vary linearly in each cell and using limited slopes; we refer here to [4] for more details.

3.2 Boundary conditions

At this stage, no specific turbulence model has been implemented at the wall. For the numerical experiments whose results are reported below, we simply weakly impose a slip condition on the two lateral boundaries.

At the inflow and outflow boundaries, the viscous fluxes are set equal to zero, and an upwind boundary condition based on the Steger-Warming flix-splitting formulation [14] is applied for the hyperbolic terms (see [5] for more details). For the inflow boundary, we see in view of (16) and (17) that this is equivalent to using an upwind formulation for the flow variables only and imposing the values of the turbulence variables k and ϵ.

3.3 Time integration method

For the time integration, we use either a fully explicit scheme (whose stability is restricted by the usual conditions on the convective and diffusive terms), of

a linearized implicit scheme (in agreement with the conclusions of the previous section). The derivation of the linearized implicit formulation follows the same lines as above in the one-dimensional case, and is described in detail in [5] (in particular, we use approximate Jacobian matrices for linearizing the hyperbolic fluxes). To simplify the algebra we do not solve implicitly the six conservative equations in a fully coupled way; instead at each time step, we first solve the linearized implicit equations for the four flow variables (the turbulent viscosity μ_t being frozen to its value at the previous time level), and then solve the equations for the turbulence variables (for simplicity, these latter two equations are linearized only with respect to the turbulence variables, the flow variables being considered here as frozen to their previous values).

As above, we use a second-order accurate approximation for the "explicit part" of the scheme (which provides in particular a second-order accurate steady-state solution if any), and a first-order accurate approximation for the implicit part, which leads to diagonally-dominant matrices and therefore facilitates the solution of the linear system to be solved at each time step. To this aim, we use point-Jacobi iterations, which allows an efficient vectorization of the computer code.

4 NUMERICAL RESULTS

As an example, we present here the numerical results obtained for a plane mixing layer test case. More precisely, we study the interaction between two parallel jets of different velocities; the velocity gradients created in the mixing zone act on the turbulence variables k and ϵ through the source term Ω. In the calculations, the Reynolds number is equal to 10000, and the inflow Mach number is 0.1.

We have used the two meshes shown on Figure 8 (the fine mesh with 600 points is twice finer than the coarse mesh, which contains 290 nodes). We compare on Figure 9 the efficiency of the first-order accurate explicit and implicit schemes on the coarse mesh; a much faster convergence is observed with the implicit scheme, which reduces by a factor of 4 the computer time needed for convergence to the steady-state solution. Figures 10 and 11 show that an efficient convergence to steady state is still observed when we move to the second-order accurate implicit scheme and to the fine mesh.

Lastly, we present the second-order accurate solution obtained on the fine mesh, with the contours of the turbulent variables k and ϵ and the

corresponding profiles along the axis (Figures 12 and 13). A comparison between the fine and coarse mesh results is shown on Figure 14. The results are in very good agreement with those of Le Ribault [11]

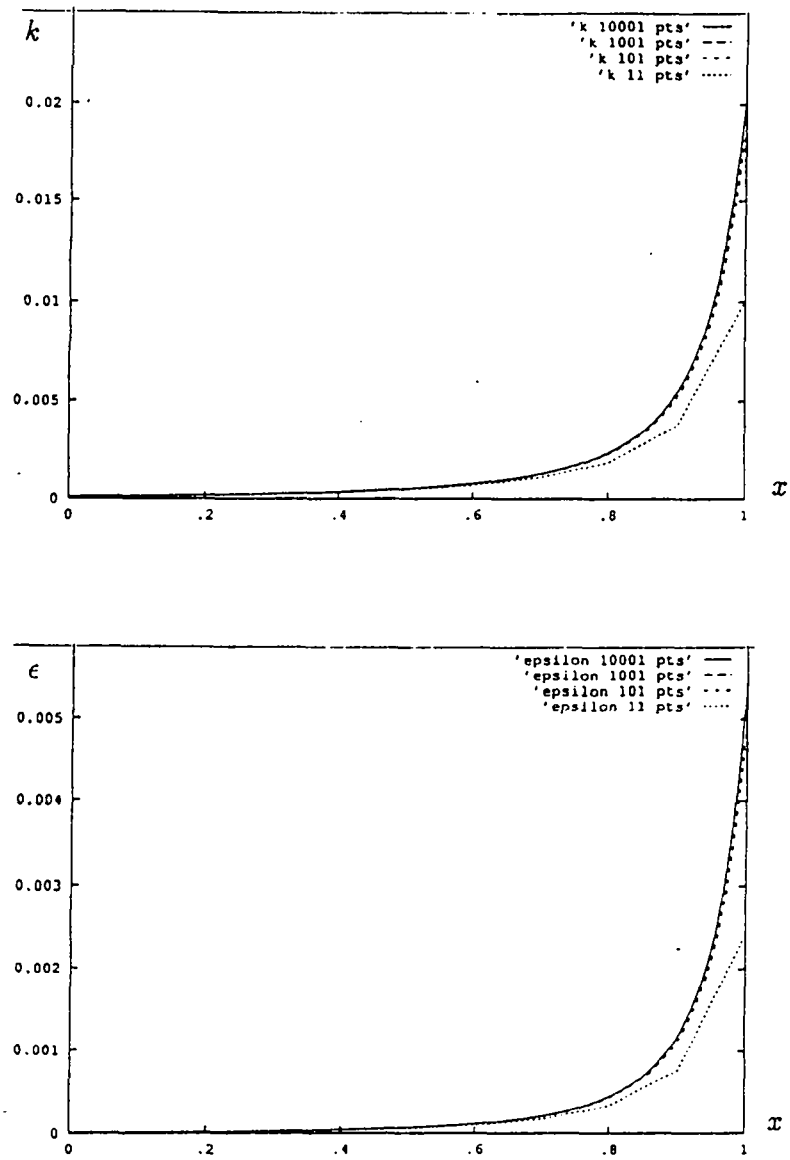

Figure 1
One-dimensional flow: profiles of the turbulent kinetic energy k and its turbulent dissipation rate ϵ.

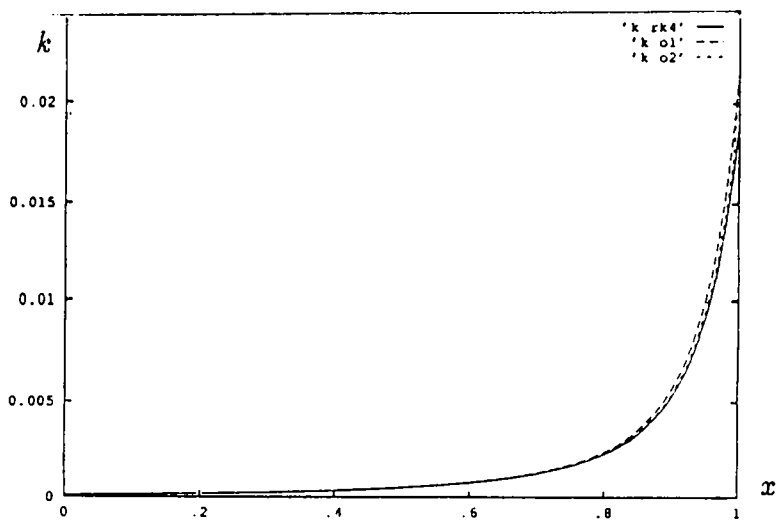

Figure 2
One-dimensional flow: comparison between Runge-Kutta 4 and explicit first- and second-order accurate schemes for k.

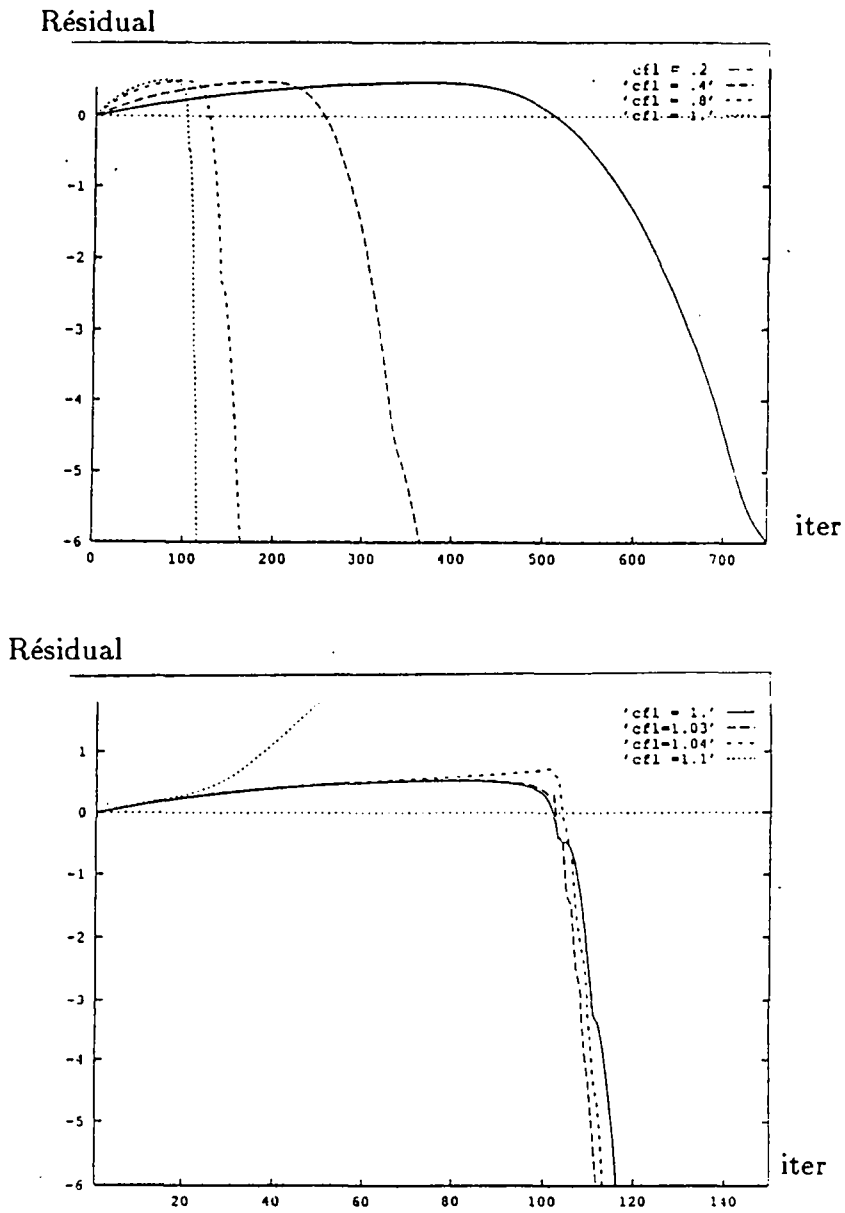

Figure 3
One-dimensional flow: convergence history for several values of the CFL number (first-order accurate scheme).

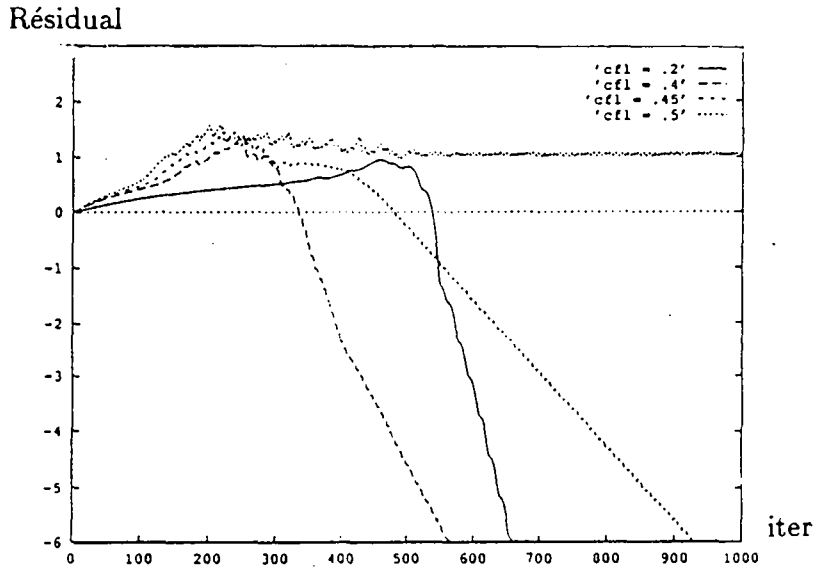

Figure 4
One-dimensional flow: convergence history for several values of the CFL number (second-order accurate scheme).

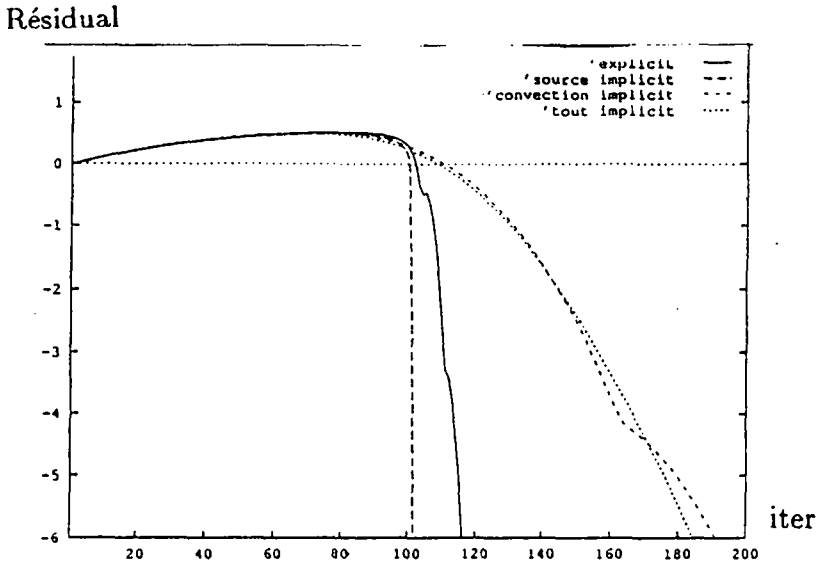

Figure 5
One-dimensional flow: comparison of convergence between explicit, semi-implicit and fully implicit schemes with a unit CFL number (first-order accurate scheme).

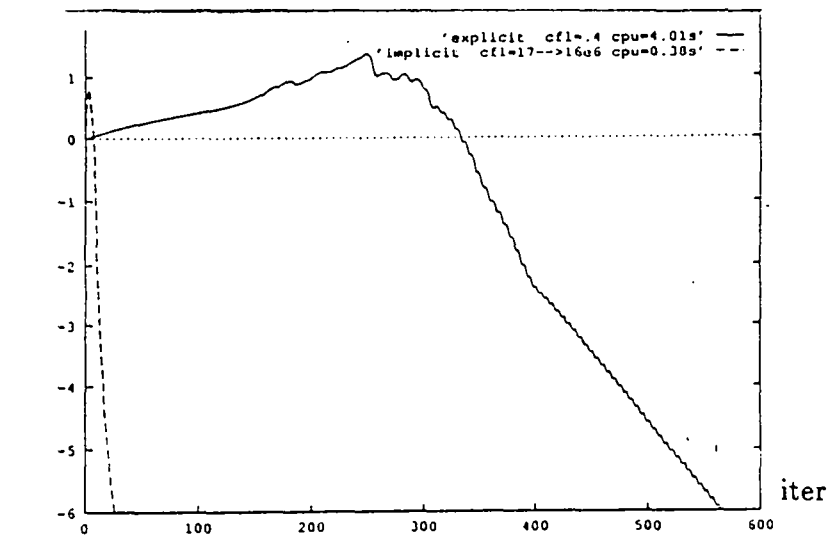

Figure 6
One-dimensional flow : comparison of convergence between the explicit scheme with a CFL number = .4, and the fully implicit scheme with variable CFL number (second-order accurate scheme).

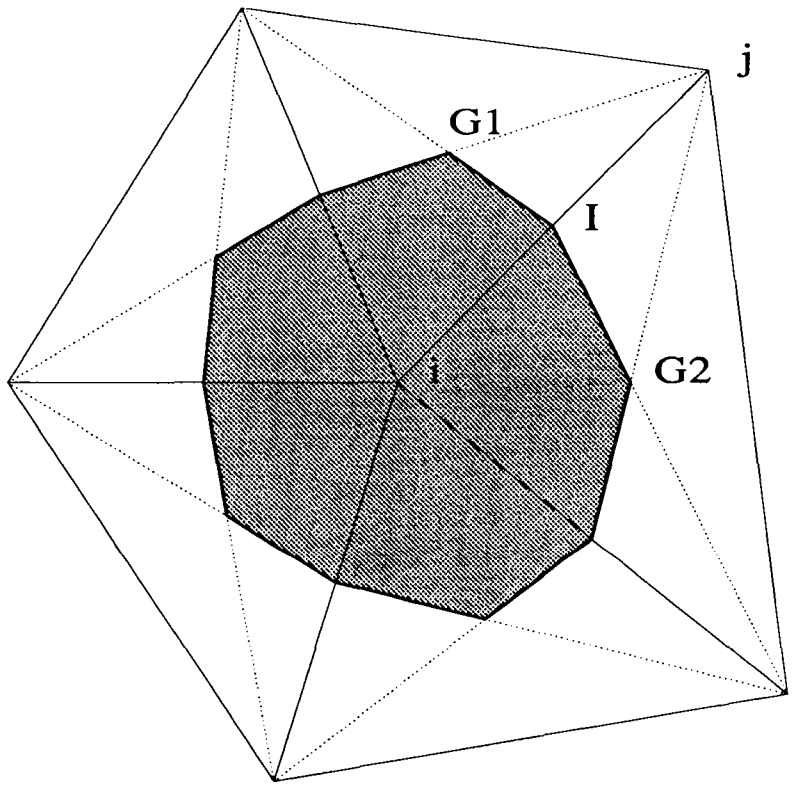

Figure 7
Two-dimensional flow: finite volume C_i.

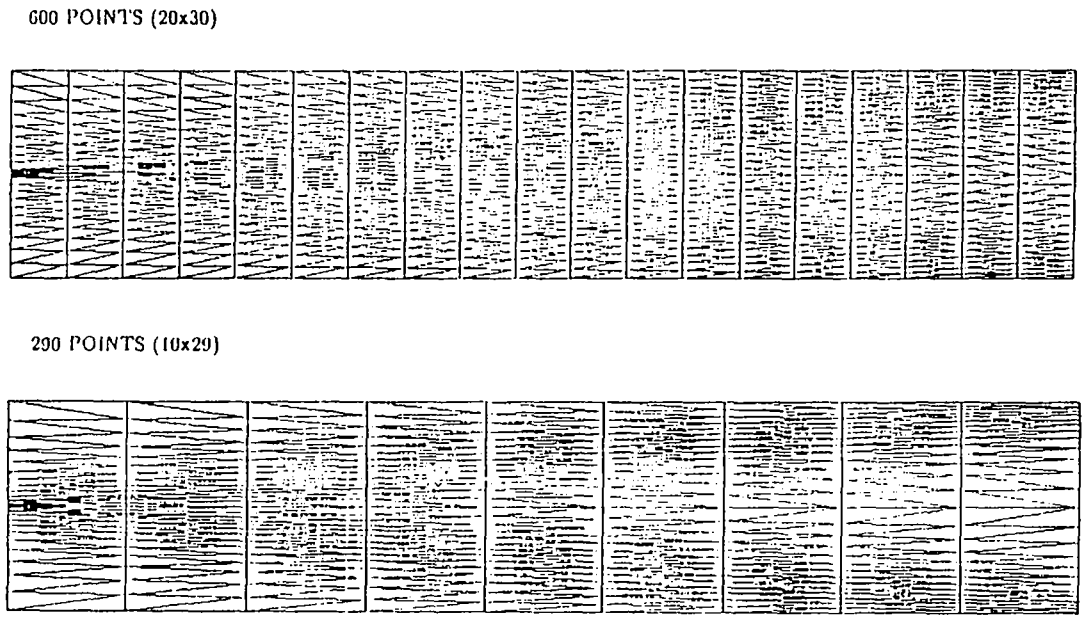

Figure 8
Two-dimensional flow: fine and coarse meshes for the plane mixing layer test-case.

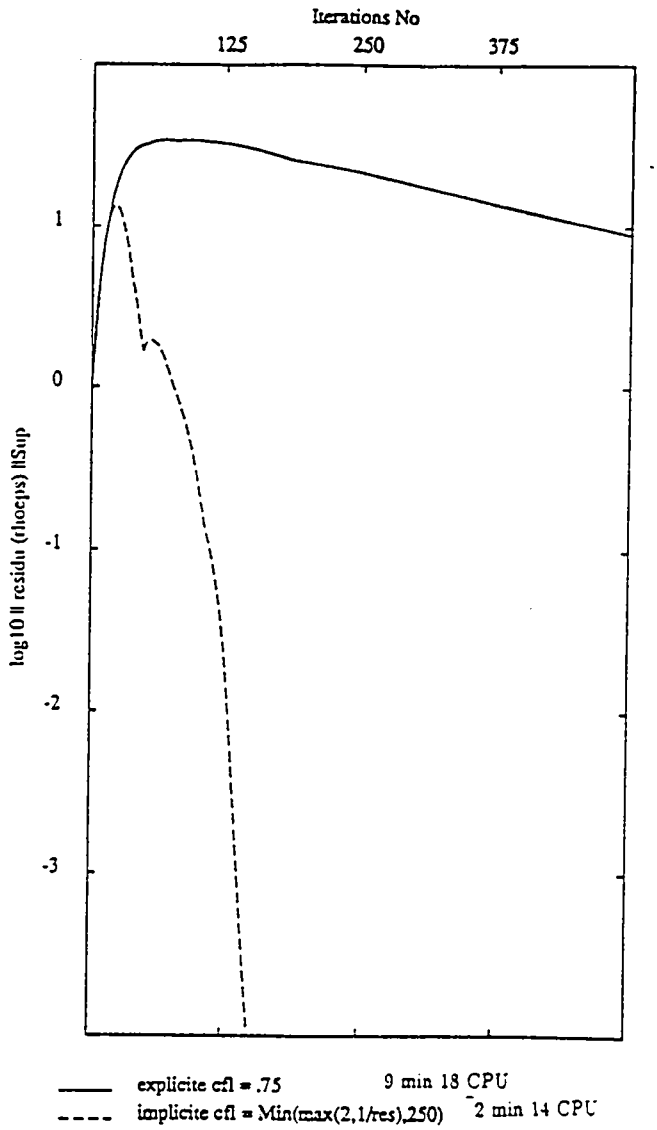

Figure 9
Two-dimensional flow: comparison of convergence between the explicit scheme and the fully implicit linearized scheme (first- order accurate scheme on coarse mesh).

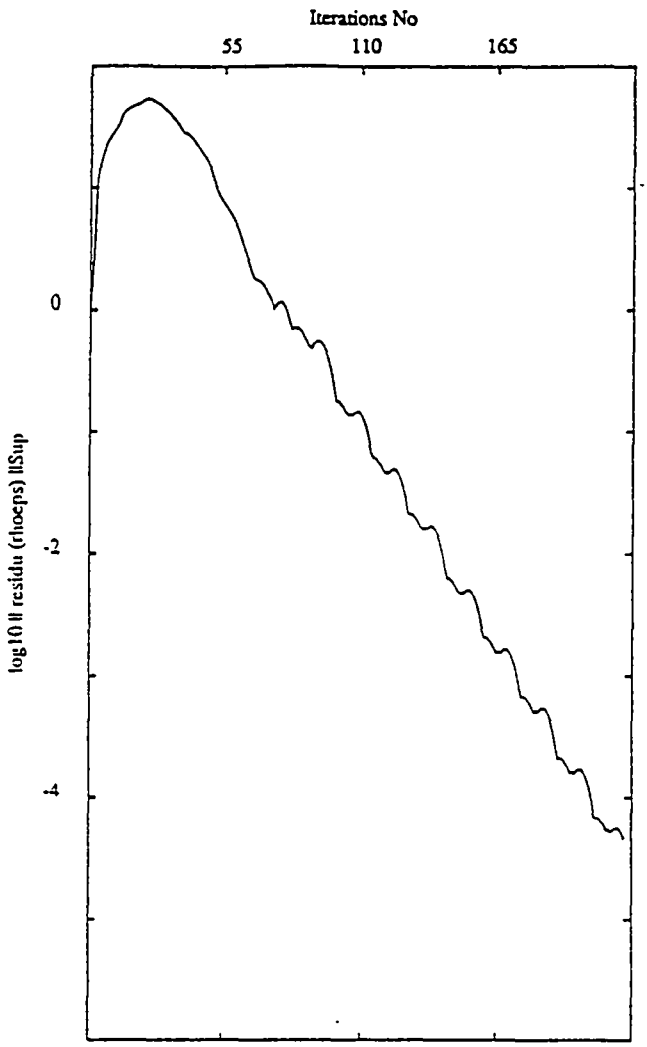

Figure 10
Two-dimensional flow: convergence history for the implicit second-order accurate scheme on the coarse mesh.

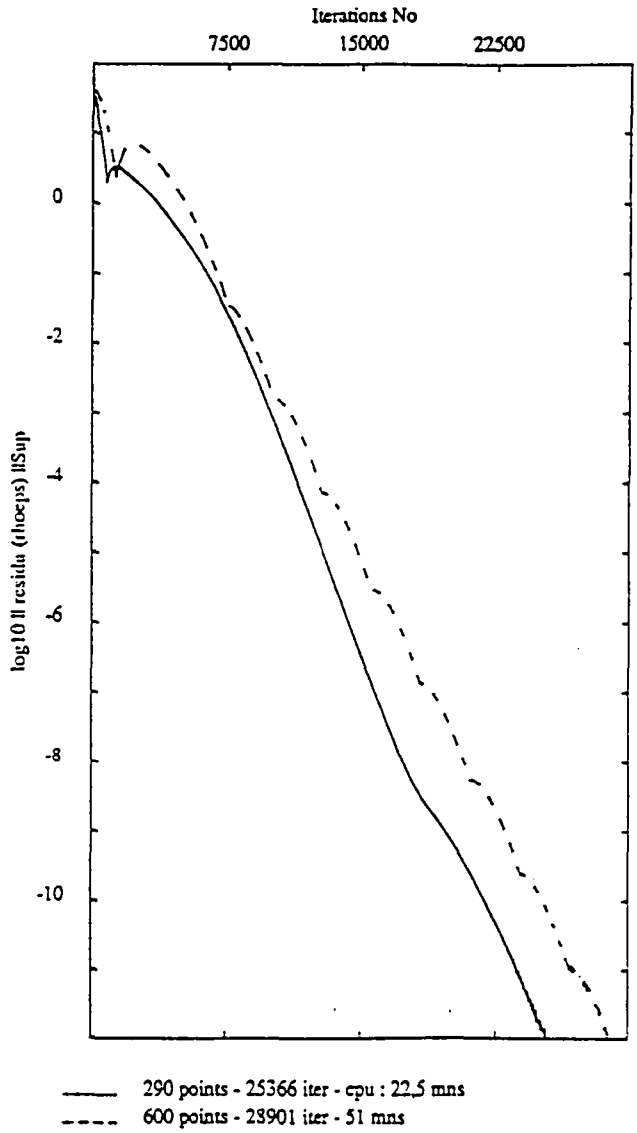

Figure 11
Two-dimensional flow: comparison of convergence on the two meshes.

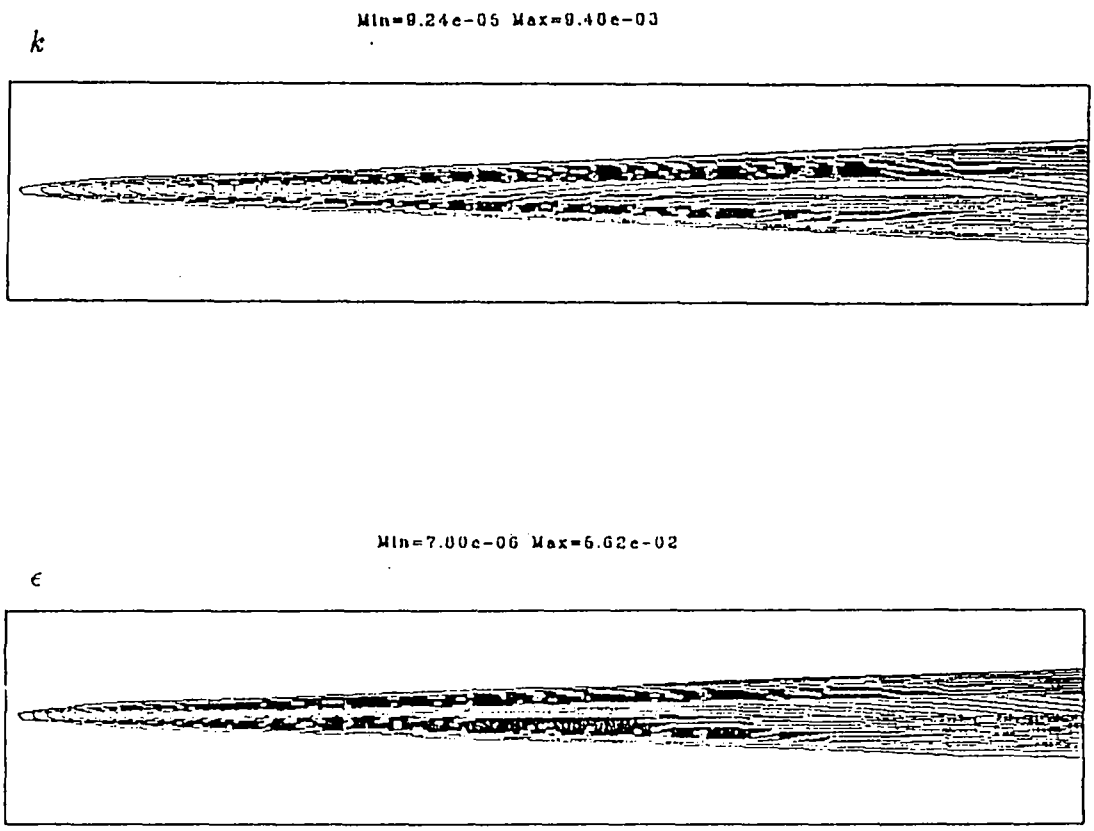

Figure 12
Two-dimensional flow: isovalues of turbulent kinetic energy k and its turbulent dissipation rate ϵ (second-order accurate scheme).

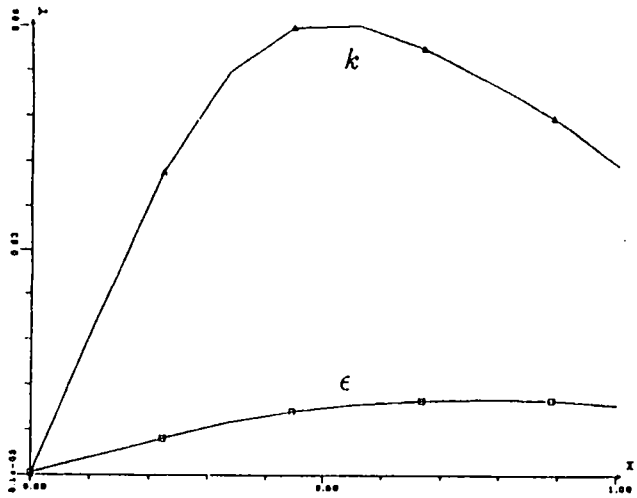

Figure 13
Two-dimensional flow: distribution along the axis for k and ϵ (second-order accurate scheme).

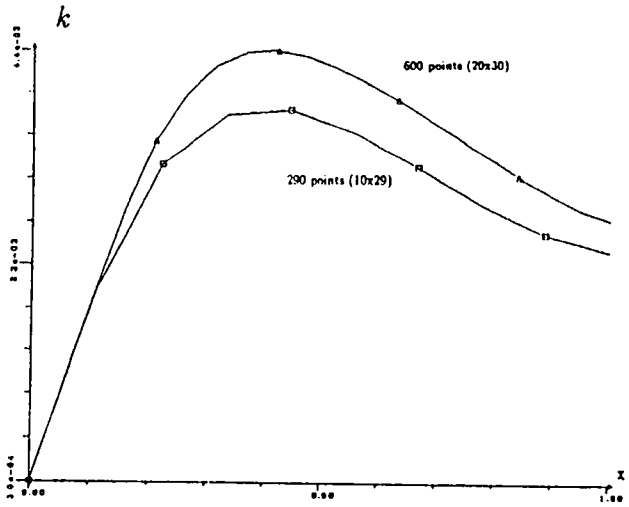

Figure 14
Two-dimensional flow: comparison of the k profile along the axis for the fine and coarse mesh (first-order accurate scheme).

5 CONCLUSION

We have presented an extension of the MUSCL–scheme to the $k - \epsilon$ model. An implicit formulation is derived from set of a 1-D numerical experiments. The conditions of a fast convergence to steady state are determined, and the linearized approach is proved to allow large time steps.

In the two–dimensional case, we have studied a similar linearized formulation. The steady 2-D problem is reduced to a series of medium–large linear systems.

The scheme is efficient and robust; some extra improvement in efficiency can be obtained by applying faster linear solution algorithms. The natural sequel of this work is to take into account wall effects; analytical wall laws are currently introduced (paper in preparation).

ACKNOWLEDGEMENTS:

This study has been developed in a common research project with Marc Buffat and Catherine Le Ribault of Ecole Centrale de Lyon; we wish to thank them and our colleague Alain Dervieux at INRIA for many helpful discussions and advices. This work was partly supported by DRET under contract 88-217.

References

[1] ANDERSON D. A. - TANNEHILL J. C. - PLETCHER R. H. , *Computational fluid mechanics and heat transfer*, Hemisphere, McGraw-Hill, (1984).

[2] CHARGY D.,DERVIEUX A., LARROUTUROU B., *Upwind adaptive finite-element investigations of the two-dimensional reactive interaction of supersonic jets* , Int. J. Num. Meth. Fluids, **11**, pp. 751-767, (1990).

[3] DERVIEUX A., *Steady Euler simulations using unstructured meshes*, Partial differential equations of hyperbolic type and applications, Geymonat ed., pp 33-111, World Scientific Singapore, (1987).

[4] FEZOUI L., *Résolution des équations d'Euler par un schéma de Van Leer en éléments finis*, INRIA Report 358, (1985).

[5] FEZOUI L., LANTERI S., LARROUTUROU B., OLIVIER C., *Résolution numérique des équations de Navier-Stokes pour un fluide compressible en maillage triangulaire*, INRIA Report 1033, (1989).

[6] FEZOUI L.,STOUFFLET B., *A class of implicit upwind schemes for Euler simulations with unstructured meshes*, J. Comp. Phys., pp. 174-206, **84**, (1), (1989).

[7] GLINSKY N., *Simulation numérique d'écoulements hypersoniques réactifs hors équilibre chimique*, Thesis, Université de Nice, (1990).

[8] A. HABBAL, A. DERVIEUX, H. GUILLARD & B. LARROUTUROU, *Explicit calculations of reactive flows with an upwind finite-element hydrodynamical code*, INRIA Report 690, (1987).

[9] LARROUTUROU B., *How to preserve the mass fraction positivity when computing compressible multi-component flows*, J. Comp. Phys., à paraître (Rapport INRIA 1080, (1989)).

[10] LAUNDER B.E., SPALDING D.B., *The numerical computation of turbulent flows*, Comp. Meth. Appl. Mech. Eng., **3**, (1974).

[11] LE RIBAULT C., Thesis, Ecole Centrale de Lyon, (1991) to appear.

[12] MOHAMMADI B., *A stable algorithm for the k-epsilon model for compressible flows*, INRIA Report 1355, (1990).

[13] ROE P.L., *Approximate Riemann solvers, parameters vectors and difference schemes*, J. Comp. Phys., **43**, pp. 357-371, (1981).

[14] STEGER J. - WARMING R.F., *Flux vector splitting for the inviscid gas dynamic with applications to finite-difference methods*, J. Comp. Phys., pp. 263-293, **40**, (2), (1981).

[15] VANDROMME D., *Contribution à la modélisation et la prédiction d'écoulements turbulents à masse volumique variable*, Thesis, Université de Lille, (1983).

[16] Van ALBADA G.D., Van LEER B., ROBERTS W.W, *A comparative study of computational methods in cosmic gas dynamics*, Astron. Astrophys., pp. 76-84, **108**, (1982).

[17] Van LEER B., *Computational methods for ideal compressible flow*, Cours von Karmann Institute, Lecture series 1983-04, Computational fluid dynamics, (1983).

Imprimé en France
par
l'Institut National de Recherche en Informatique et en Automatique.

ISSN 0249 - 6399